Proceedings of the ASME 2010 3rd Joint US-European Fluids Engineering Summer Meeting and 8th International Conference on Nanochannels, Microchannels, and Minichannels
FEDSM-ICNMM2010
August 1-5, 2010, Montreal, Canada

FEDSM-ICNMM2010-30835

STUDY OF THE IMPACT OF CHANGE OF CLEARANCE ON THE FLOW FIELD AND ROTORDYNAMIC COEFFICIENTS FOR A SMOOTH, WHIRLING ANNULAR SEAL

Aarthi Sekaran
Texas A&M University
College Station, TX, USA

Dr. G. L. Morrison
Texas A&M University
College Station, TX, USA

ABSTRACT

The flow field and the rotordynamic coefficients for a smooth, whirling annular seal were investigated by means of a CFD study involving a full 3D model. The preliminary model (of clearance 1.27mm) was validated by comparison to existing experimental flow field data after which CFD simulations were made for a smaller clearance (0.127mm). The flow field changed significantly with the change in clearance and it was seen that the larger clearance showed an inertia dominated flow regime as opposed to the viscous flow regime for the small clearance. Upon the implementation of Childs' theory for the computation of rotordynamic coefficients, it was observed that forces for the larger clearance did not exhibit the whirl ratio dependence assumed in this theory. The smaller clearance however showed the expected trend with values of the coefficients in the range predicted.

INTRODUCTION

Annular seals, although primarily used for leakage control, have a substantial impact on the stability of a turbomachine. This makes investigation of the flow field and the resulting forces exerted on the rotor an essential research subject in the field of turbomachinery. Although the geometry of smooth annular seals is relatively simple, the high pressure difference across the seal can lead to highly turbulent flow regimes. The flow field influences the forces generated by the seal which change with the positions of the rotor results. These forces may provide stabilizing or destabilizing effects. Whirling motion may contribute towards stabilizing or destabilizing the system, depending on the characteristics of the seal, its operating condition and the orbit path of the rotor.

There have been extensive experimental studies involving annular seals, and a significant number of them have been conducted at the Turbomachinery Laboratory at Texas A & M University. These experimental data include 3D LDA measurements of the velocity along with various parameters such as the pressure and the wall shear stress, for a range of flow conditions. There are also complementing numerical studies for annular seals but these are mainly limited to studying the rotordynamic coefficients using bulk flow models. The need for a more intensive numerical study stems from the fact that the range of experimental parameters that can be varied in an experimental facility is limited by resources. Another drawback of using an experimental method is that measured data is accessible at a restricted number of positions on the seal and not over the entire surface, as in case of a CFD study.

The present study develops a full 3D CFD model for smooth annular seals which can be applied for seals whirling in various orbits. The solver used for this analysis is FLUENT (Ver. 6.3.26) and the model is created in GAMBIT (Ver. 2.4.6). The selection of the solver is linked to its capability to use a time-dependent module to simulate the whirling motion. This was accomplished using a dynamic meshing application in conjunction with user defined functions (to specify orbit paths).

NOMENCLATURE

C	Direct damping coefficient
c	Cross-coupled damping coefficient
e	Eccentricity
F_r	Radial force
F_t	Tangential force
F_x	Horizontal force
F_y	Vertical force
K	Direct stiffness coefficient
k	Cross-coupled stiffness coefficients
L	Seal length
M	direct mass coefficient
m	Cross-coupled mass coefficients
R	
Re	Reynolds number
Ta	Taylor number

X Horizontal direction
Y Vertical direction
Z Axial distance from seal inlet
κ Turbulent kinetic energy
ε Turbulent dissipation rate
Ω Whirl ratio

METHODOLOGY

The full 3D models used for this study are constructed based on the seal geometry from prior experimental studies [1, 2]. The seal with the larger clearance of 1.27mm, is modeled in accordance with that used by Johnson [1] and Thames [2] as one of the initial goals is to validate the CFD model by comparing the results to those obtained experimentally. The dimensions are as follows: L=37.3mm, R=82.05mm and clearance c = 1.27mm (50mil). The whirl orbit radius is one half of the clearance and the rotor was maintained at an eccentricity ratio of 50%, resulting in a circular orbit.

The entire model is meshed using a hexahedral scheme and the final mesh having approximately 1,000,000 nodes. The economy of the mesh was ensured by using a very fine mesh close to the clearance region and a reasonable mesh quality over the remainder of the seal. Fig. 1 shows a representative mesh while Fig. 2 shows the results of a grid independence study. Since the region of interest is in the clearance of the seal, it is the number of nodes (along the radial direction) in this region that was varied to obtain grid independence.

Once the model is created, the next step is to simulate the whirling motion of the rotor. This is accomplished using dynamic meshing in FLUENT. Dynamic meshing essentially accounts for changes in shape of the domain which are computed and updated at every time-step. The orbit paths (which affect the unbalanced forces on the rotor) are specified by user defined functions. User defined functions are basically programs written in C++ which serve the purpose of customizing certain modules of the commercial code. For this study, UDFs were applied to simulate various orbit paths.

The standard $k-\varepsilon$ turbulence model is implemented along with the enhanced wall treatment with pressure- gradient affects. Although the $k-\varepsilon$ model has been proven to be effective for turbulent core flows, it is also essential to have an accurate model for the near wall regime (as applicable to the moving rotor wall) and this was accomplished by the use of the enhanced wall treatment. The pressure gradient effect was also used in order ensure accuracy through the variation of clearances from the seal inlet to the outlet.

The working fluid used for the study is water with the properties as in the FLUENT database. A shaft speed of 3600 RPM (corresponding to a Taylor number of 6600) was used and the flow was specified by a mass flow rate of 4.87 kg/s (for a Reynolds number of 24000). In order to study the effect of the clearance, a seal with one-tenth the clearance of the initial seal was modeled while keeping the rest of the dimensions the same (the results of a grid independence study are shown in Fig. 3). The boundary conditions used are also based on the previous model as there is no experimental data to compare for this case. The mass flow rate used was one-tenth of that used earlier i.e. 0.487 kg/s and this was done in order to ensure the same axial velocity for both cases. The other non-dimensional parameters are correspondingly reduced to a Reynolds number of 2400 and Taylor number of 208.

RESULTS

FLOW FIELD COMPARISONS

The results for the flow fields from the simulations have been presented by obtaining 'slices' of the seal at various axial locations and then magnifying these slices in order to clearly observe the contours. The locations of these axial slices were based on the experimental data available in order to facilitate one to one comparisons and the locations are presented as fractions of the total axial length of the seal (37.3mm).

The slices have been taken at Z/L = 0.036, 0.11, 0.22, 0.77 and 0.86 (where L is the length of the seal section, 37.3 mm) conforming to the LDA data available. The results are presented in Figs. 5(a)-(e). The LDA data has been interpolated from the measured values which could not be taken at all angular locations.

At the slice Z/L = 0.036, the axial velocity contours are predicted almost exactly by the simulations. The regions of high and low velocities and their locations are reproduced quite accurately, the only discrepancy being that the area of low velocity is slightly larger in case of the predictions. This region of low velocity which is seen at the maximum clearance shows a region of stagnant flow which could be the wake of the sudden step in the inlet region. For the contours of radial velocity, the values are identical in case of both the simulations and measurements; however, the location of the region of low velocity as seen in the simulations is different from that seen in the LDA data. Also, observing radial velocity vectors indicates that they point outward near the rotor and inward close to the maximum clearance position on the stator which is the characteristic of a vena contracta. The tangential velocity is under-predicted by the simulations; the areas of high and low velocity are however reproduced correctly. The maximum discrepancy is seen at the region of maximum clearance which also holds for the predictions for the statically eccentric seal. Also, it is seen that the thin boundary layer close to the rotor surface was not captured by the LDA measurements but is clearly seen in the simulations.

The slice at Z/L=0.11 follows the same trends as the previous slice. The profile in general is more evenly distributed owing to the region of maximum velocity moving to a wider clearance, which decelerates the flow. The radial velocity contours again show good agreement while the contours of tangential velocity show an under-prediction as in case of the previous slice. The tangential velocity contours show a slight overall increase due to the rotor tangential shear stress continually accelerating the azimuthal velocity as the flow progresses through the seal.

For the next slice at Z/L = 0.22, the axial velocity contours from the measured values again show a significant drop in small clearance values as opposed to the more gradual decrease in case of the predictions. Also, the predictions show a small region of zero velocity very close to the rotor which is absent in the experimental data and this could be attributed to the fact that LDA data very close to a surface is hard to obtain. The radial velocity values are relatively lower than the tangential and axial velocities as in the previous observations and these contours show overall agreement except close to the region of minimum clearance where the values are slightly lower for the predictions.

The next axial slice at Z/L = 0.77 shows little variation in the axial velocity around the circumference for the LDA data. This is however not the case for the simulated results which shows a significant change from the previous slice at Z/L=0.22 - a region of high velocity is seen to develop on the lower half of the pressure side (close to the maximum clearance region), the magnitude of which is much higher than that seen for the previous slice. The radial velocity comparisons show relatively better agreement except for the small region of slightly high velocity which is not seen in the simulated results. The tangential velocity contour comparisons are more accurate that for the previous slices and the overall distributions and ranges of velocity are relatively similar.

The same trends as for the slice at Z/L=0.77 are repeated in case of the slice at Z/L = 0.86. The axial velocity contours are overall under-predicted by the simulations which do however follow through the distributions seen over all the other slices. The radial velocity fields are again well reproduced except for the location of the region of low velocity which is at the minimum clearance in case of the simulations. The tangential velocity contours show better agreement here than in the initial slices, the distributions are almost identical but the measured values do show a slightly higher value of maximum velocity in a few small locations.

Upon studying the flow fields over all the slices, it is possible to make a few conclusions regarding the physics of the flow. It is seen that the axial velocity shows maximum values at the entrance of the seal, on the pressure side and rotates circumferentially to the suction side at the exit. The tangential velocity on the other hand develops with almost a reverse trend, i.e. the values are lower at the entrance and slowly build up towards the exit. Overall, the predictions agree with the data to a fair extent. To obtain highly accurate results, it might be necessary to investigate other turbulence models or use a much finer grid with an LES scheme. This is confirmed by studying the pressure variations over the rotor surface as seen in Fig 4 which shows that although the overall trend of the variation is captured, the CFD data is unable to capture the small scale variations.

COMPARISON OF 5 AND 50 MIL CLEARANCE SEALS

Fig. 6(a) shows the axial, radial and the tangential velocity contours for the seals with 5 and 50 mil clearances operating with a 50% eccentricity ratio and a whirl ratio of 1. These results are taken at an axial location of Z/L = 0.036 which is close to the inlet of the seal. The axial velocity contours show similar ranges for both clearances and this is to be expected from the fact that the mass flow rates were chosen accordingly. The variation in flow behavior is however noticeable – the larger clearance shows the region of maximum velocity in the minimum clearance region while for the smaller clearance this region is closer to the maximum clearance region. A more significant impact of the change in clearance is seen upon comparing the tangential velocity contours. The magnitudes of tangential velocities seen are clearly larger in magnitude for the seal with 5mil clearance; also, the location of the maximum velocity region is a thin layer close to the rotor for the large clearance while the smaller clearance shows the maximum velocity in the minimum clearance region.

Studying the flow moving deeper into the seal, at Z/L = 0.11, similar trends for the axial velocity contours are seen to continue for both seals. The maximum velocity region is also observed to spin in the anti-clockwise direction which is the direction of rotation of the rotor. The radial velocities show very low magnitudes with almost identical distributions over the entire length of the seal, indicating that this component of the velocity shows little impact of the change in clearance. The tangential velocity contours for the 5mil seal show a marked development unlike that of the larger clearance thus clearly showing the impact of the change in clearance.

Axial slices at Z/L = 0.22 and Z/L = 0.77 show the axial and radial velocity contours slowly continuing to grow by the same trends seen so far. Observing the 5mil seal at this stage shows the tangential velocities developing and the maximum velocity region spanning the entire minimum clearance region of the seal. The slice at Z/L = 0.77 shows the flow to be nearly fully developed with the maximum velocity region

ROTORDYNAMIC COEFFICIENTS

The determination of the rotordynamic coefficients was the other significant part of this study. Using Childs' theory [3], for small radial displacements about the rotor's arbitrary positions, the reaction forces F_x and F_y can be modeled as

$$-\begin{bmatrix}F_x\\F_y\end{bmatrix} = \begin{bmatrix}K_{xx} & K_{xy}\\K_{yx} & K_{yy}\end{bmatrix}\begin{bmatrix}x\\y\end{bmatrix} + \begin{bmatrix}C_{xx} & C_{xy}\\C_{yx} & C_{yy}\end{bmatrix}\begin{bmatrix}\dot{x}\\\dot{y}\end{bmatrix} + \begin{bmatrix}M_{xx} & M_{xy}\\M_{yx} & M_{yy}\end{bmatrix}\begin{bmatrix}\ddot{x}\\\ddot{y}\end{bmatrix}$$

where $x, \dot{x}, \ddot{x}$ and $y, \dot{y}, \ddot{y}$ are the displacements, velocities and accelerations in the x and y directions. When the nominal position of the rotor is concentric with respect to the housing, the coefficient matrix becomes simper and assumes a skew-symmetric form -

$$-\begin{bmatrix}F_x\\F_y\end{bmatrix} = \begin{bmatrix}K & k\\-k & K\end{bmatrix}\begin{bmatrix}x\\y\end{bmatrix} + \begin{bmatrix}C & c\\-c & C\end{bmatrix}\begin{bmatrix}\dot{x}\\\dot{y}\end{bmatrix} + \begin{bmatrix}M & m\\-m & M\end{bmatrix}\begin{bmatrix}\ddot{x}\\\ddot{y}\end{bmatrix}$$

where K and k are the direct and cross-coupled stiffness coefficients, C and c are the direct and cross-coupled damping coefficients and M and m are the direct and cross-coupled mass coefficients.

In order to relate these forces to the data obtained from the CFD study, the method adopted by Xi and Rhode [4] was followed. According to this study, once the simulations are converged and the resulting tangential and radial force components are obtained for various circular orbit whirl ratios, the components are related to the rotordynamic coefficients by

$$\frac{-F_r}{e} = K + c\Omega - M\Omega^2$$

$$\frac{-F_t}{e} = -k + C\Omega + m\Omega^2$$

This is used in conjunction with a least squares curve fitting with respect to whirling speed to obtain the rotordynamic force coefficients. The simulations for both the 5 and 50 mil clearance seals were performed for whirl ratios from 0 to 1 for a 50% eccentricity ratio circular orbiThe radial and tangential impedances obtained along with the curve fits for the 50mil seal are shown in Fig.7. It is seen that the radial force initially exhibits a decrease in magnitude from whirl ratios 0 through 0.4 after which an increase is seen from 0.4 through 0.8. This is then followed by a slight drop from 0.8 to 1.0. The initial decrease in force is seen to be consistent with the decrease in pressure variations for these whirl ratios. The increase from whirl ratios 0.4 to 0.8 however, takes place even though the pressure variation remains constant, indicating that there must be a change in the pressure distribution which causes it.

As seen from the plot, the data does entirely conform to a second order polynomial. This discrepancy could be attributed to the fact that the simulations may be unable to capture the presence of Goertler vortices which are formed along the axial flow direction and may need to be investigated further. The variation of the forces with whirl ratio for the 5mil case is shown in Fig.8. The initial observation made is that the magnitudes of the forces are smaller than that seen in case of the large clearance seal. The radial forces at first follow the trend seen earlier with the decrease in magnitude from whirl ratios 0 through 0.4. From 0.4 to 1.0 however, the expected trend of increase is seen hence leading to the attainment of a second order polynomial that conforms to Childs' theory.

The tangential force distribution is shown in Fig. 8(b), and like the radial forces, they initially show the same trend as the 50mil case; the magnitudes however are larger. Past a whirl ratio of 0.2, the force components which were seen to initially decrease and then increase in case of the 50mil clearance are seen to uniformly increase for the 5mil case. This is the effect of the larger radial and tangential velocities which were observed in the flow field of the case of the small clearance. The effect of the 'damping' was seen in this case as well leading to a smaller variation in the magnitude of forces.

Studying the variation of forces for both the clearances in conjunction with previous studies, it is seen that the discrepancies observed can be explained. The experimental results from Kanemori and Iwatsubo [5] could help justify the results obtained here and this data was also used by Xi and Rhode [4]. The first observation made is that the simulations performed for the former case were for a clearance of 0.394mm as compared to the 1.27mm (50mil) that was done for this study – this indicates that the theory may not hold for large clearances and it might be necessary to investigate alternate methods to determine the rotordynamic coefficients. The other differences seen are in terms of the pressure drops and the axial Reynolds numbers where the values used by Kanemori and Iwatsubo for both these factors were much lower than those for the 50mil case in the present study.

CONCLUSION

A full 3D CFD model for smooth annular seals was developed along with a method to simulate the whirling motion of seals. Flow field comparisons were made by applying this concept to two different clearances of 50mil and 5mil and the characteristics of the flow field varied considerably for both seals. The smaller clearance showed a viscosity dominated behavior while for the large clearance an inertia dominated flow regime was observed. The differences in the flow fields also carry over for the determination of rotordynamic coefficients – it was observed that while the large clearance showed forces that deviate from the expected trend (as predicted by Childs) the smaller clearance showed forces that follow the predictions. This hints that the theory applied may be limited to small clearances and the application of the theory would need a closer investigation.

ACKNOWLEDGMENTS

This work was sponsored by the Turbomachinery Research Consortium, Turbomachinery Laboratory, Texas A&M University, College Station, Texas

REFERENCES

1. Johnson, M.C., 1989, "Development of a 3-D Laser Doppler Anemometry System: With Measurements in Annular and Labyrinth Seals," PhD Dissertation, Texas A&M University, College Station.
2. Thames, H. D., 1992, "Mean Flow and Turbulence Characteristics in Whirling Annular Seals," M.S. Thesis, Texas A&M University, College Station.
3. Childs, D.W., 1982, "Finite-Length Solutions for Rotordynamic Coefficients of Turbulent Annular Seals," ASME J. Lubrication Technology, **105**, pp. 429-436.
4. Xi, Jinxiang and Rhode, D. L. (2006) "Seal-Inlet Disturbance Boundary Condition Correlations for Rotordynamics Models, Part 2: Assessment," Tribology Transactions, **49** (4), pp.584 -591.
5. Kanemori, Y. and Itwatsubo, T., 1989, "Experimental Study of Dynamical Characteristics of a Long Annular Seal," JSME International Series II, **32**, pp. 218-224.

ANNEX A

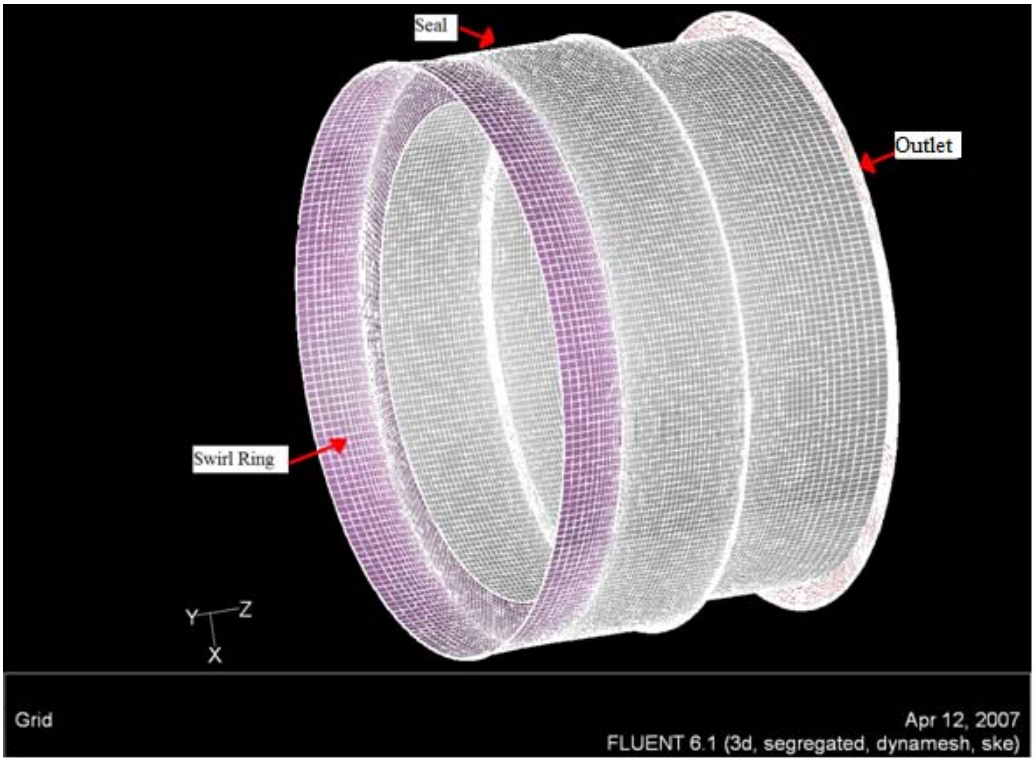

Fig.1- Meshed seal geometry

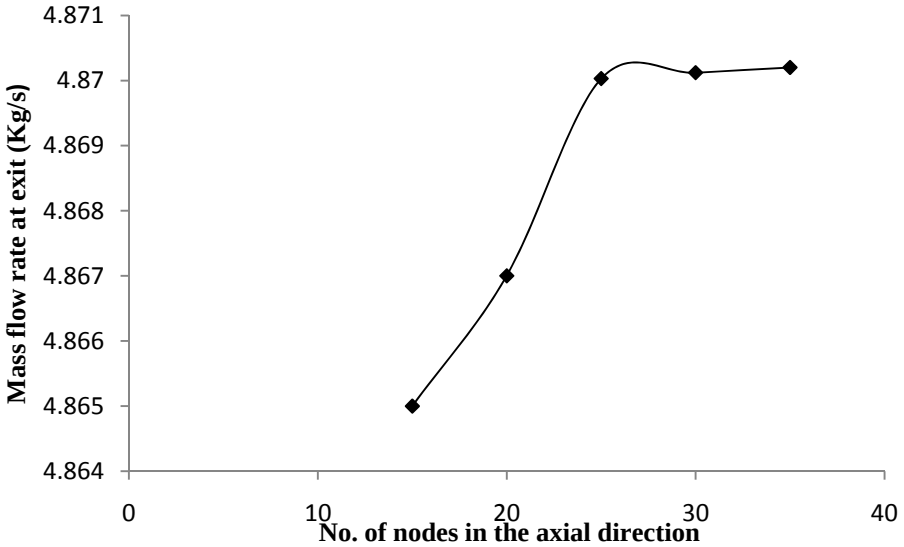

Fig.2- Grid Independence study for 50mil seal

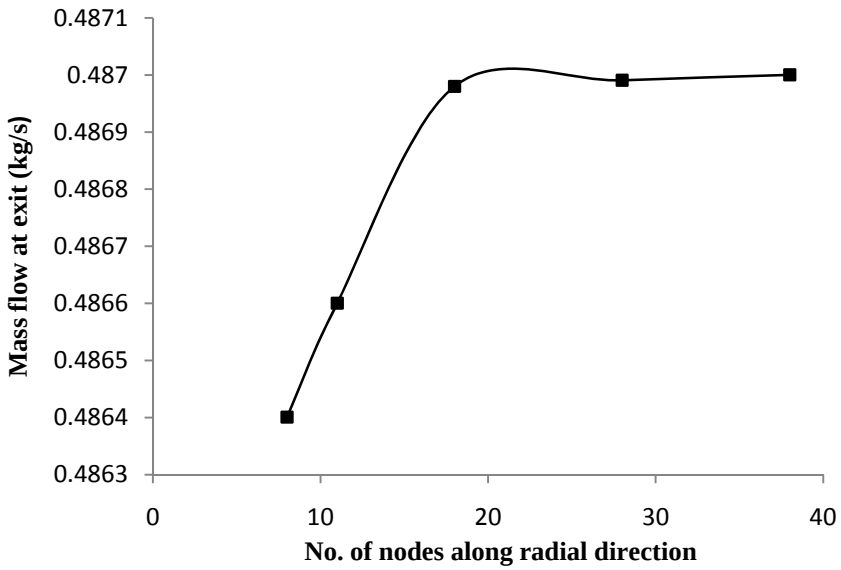

Fig.3 - Grid Independence study for 5mil seal

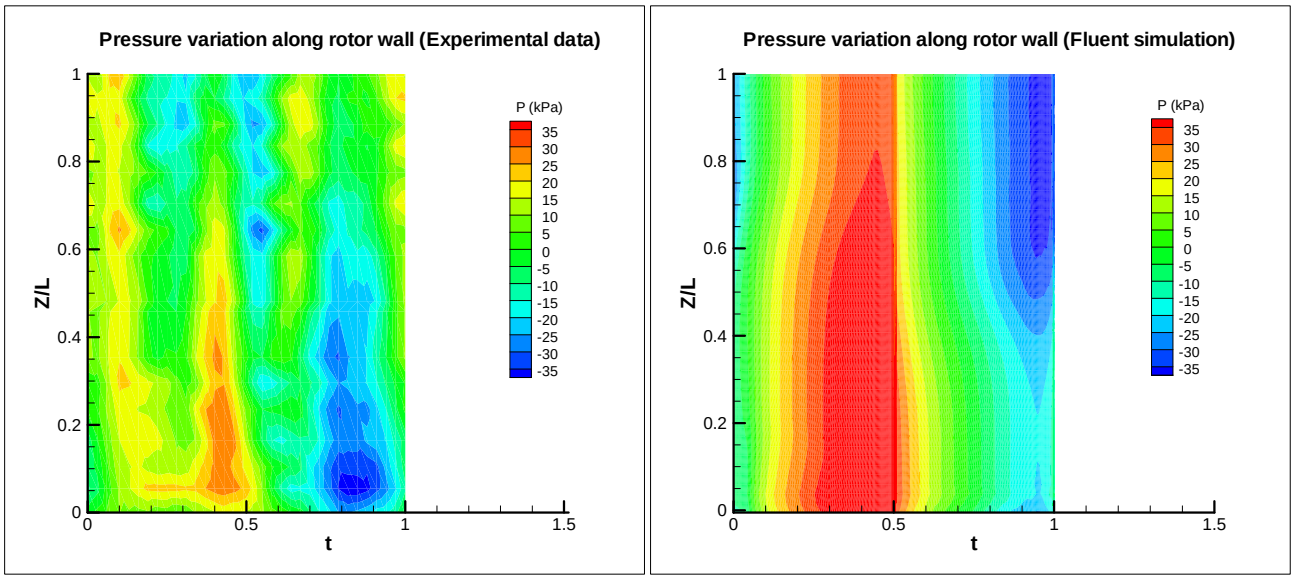

Fig.4 - Comparison of variation of pressure along the length for experimental and CFD data for the 50mil seal

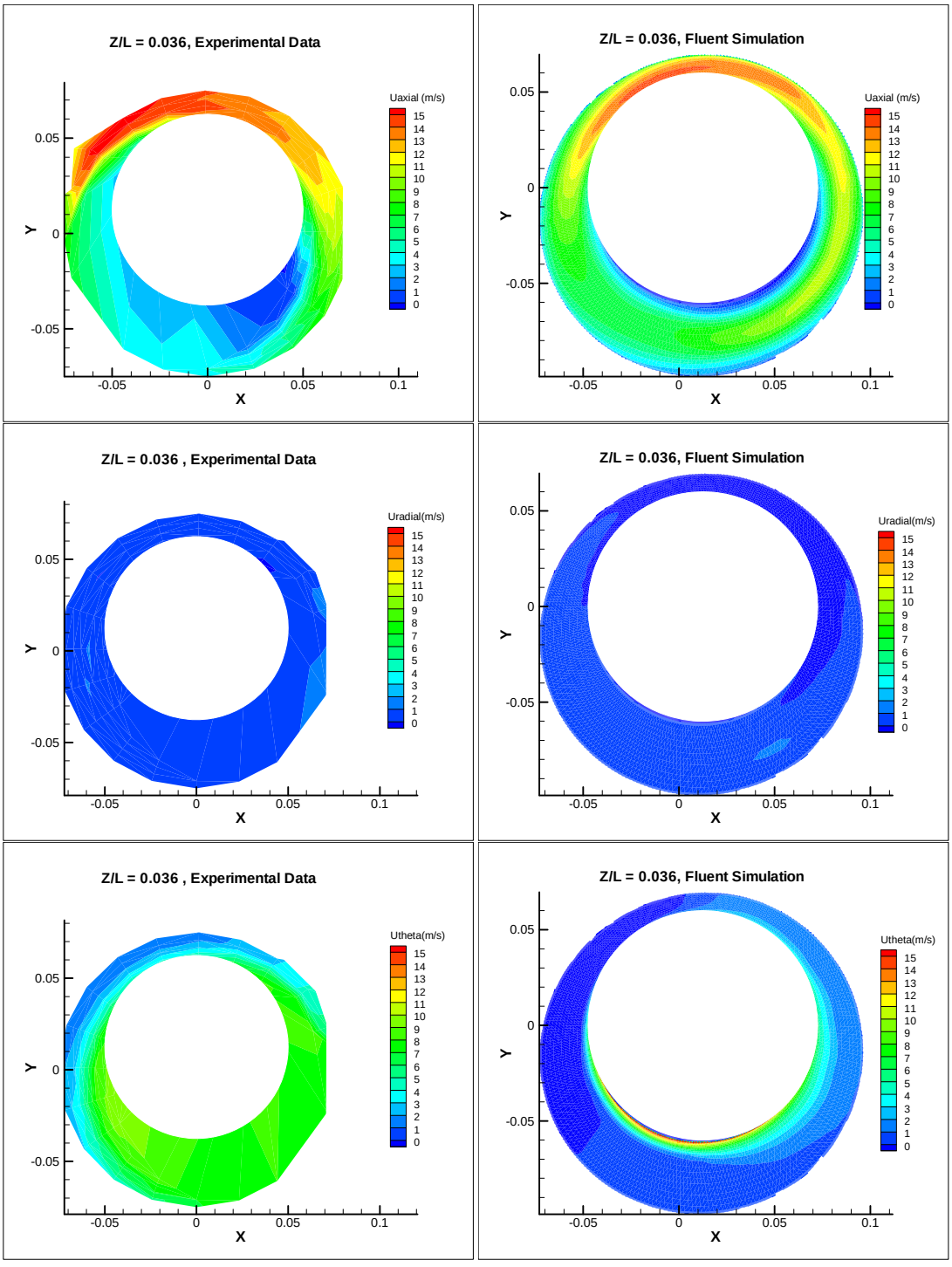

Fig.5 (a) LDA data and FLUENT simulation results for Z/L = 0.036

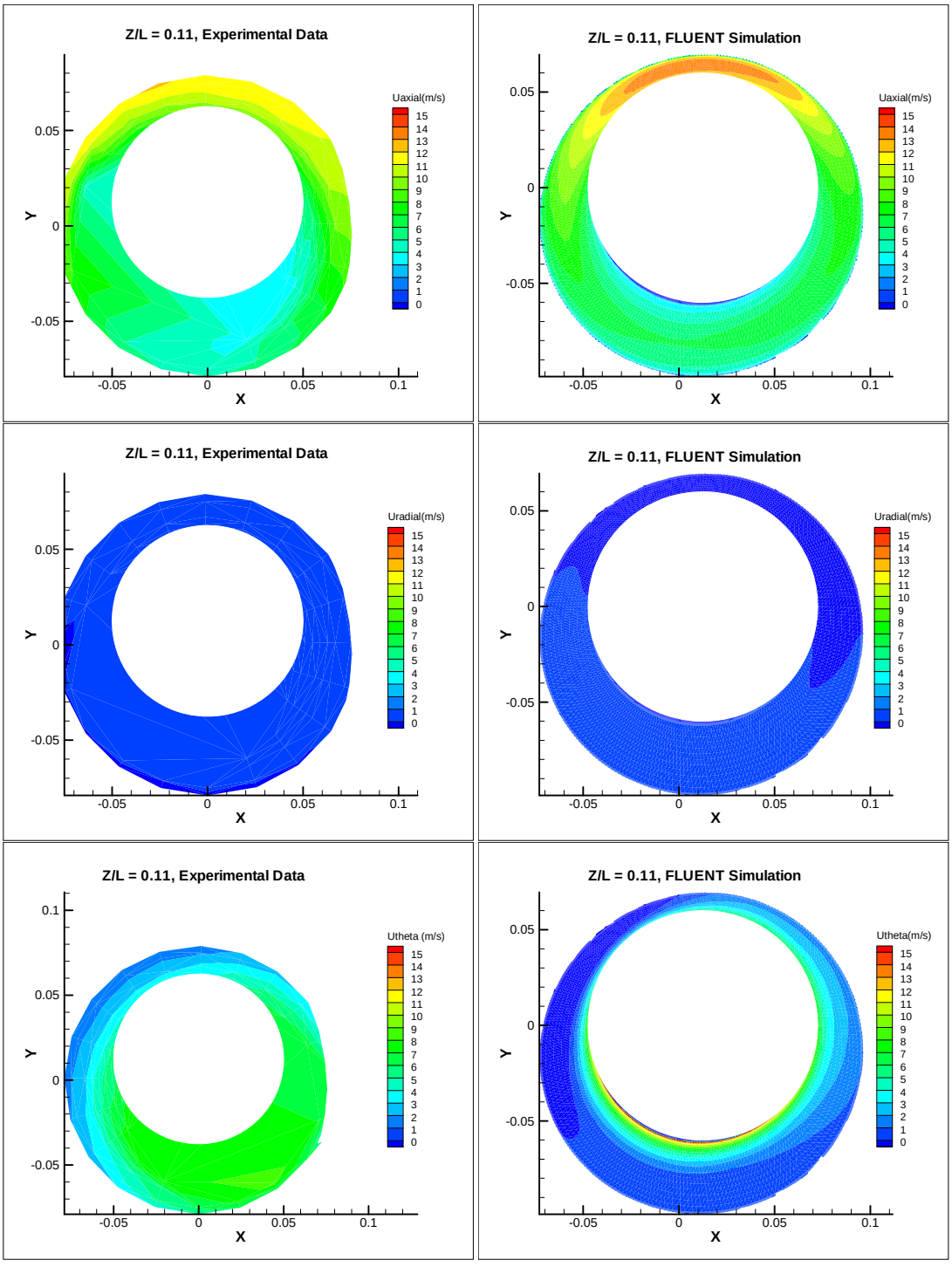

Fig. 5 (b) LDA data and FLUENT simulation results for Z/L = 0.11

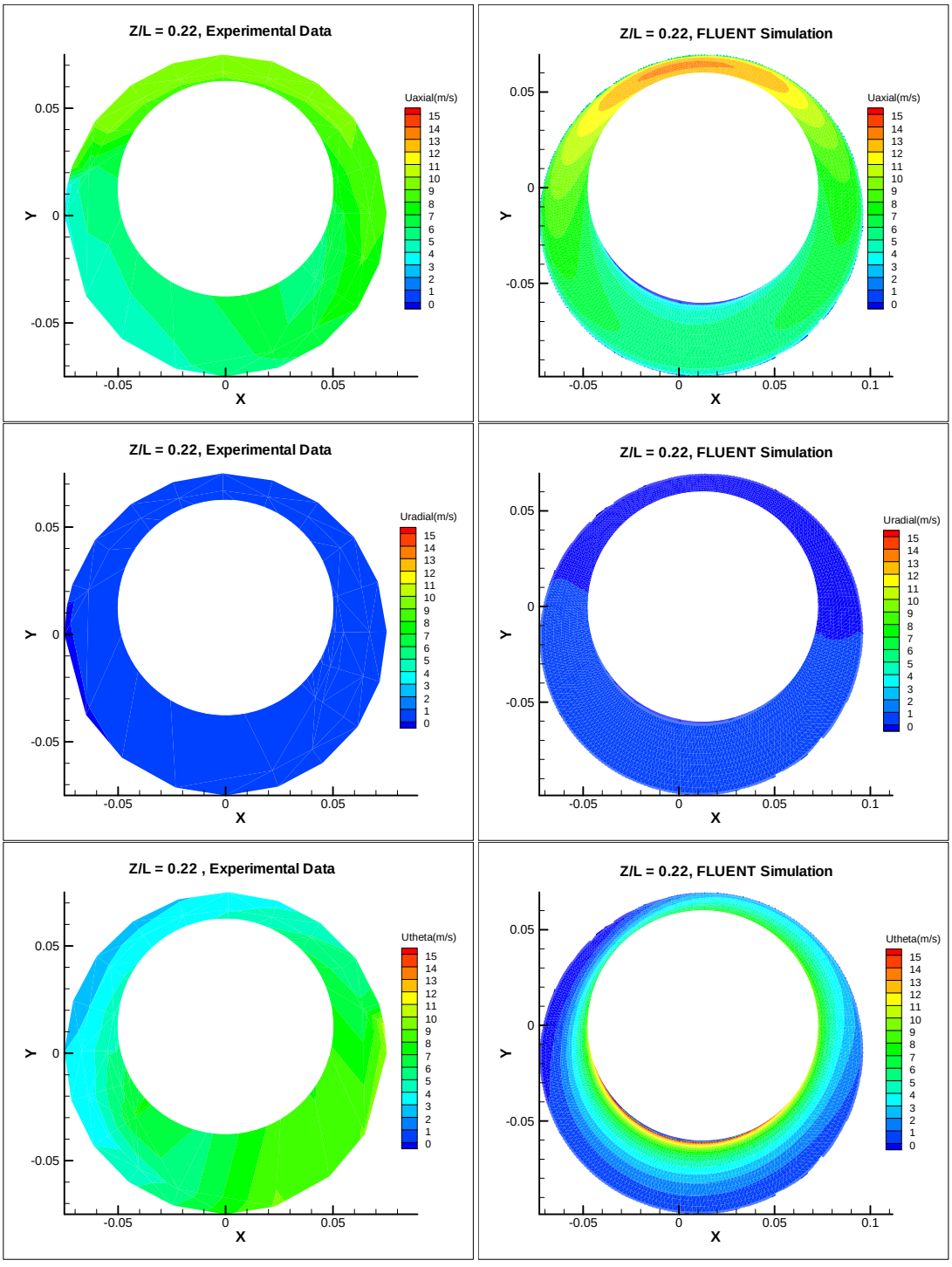

Fig. 5 (c) LDA data and FLUENT simulation results for Z/L = 0.22

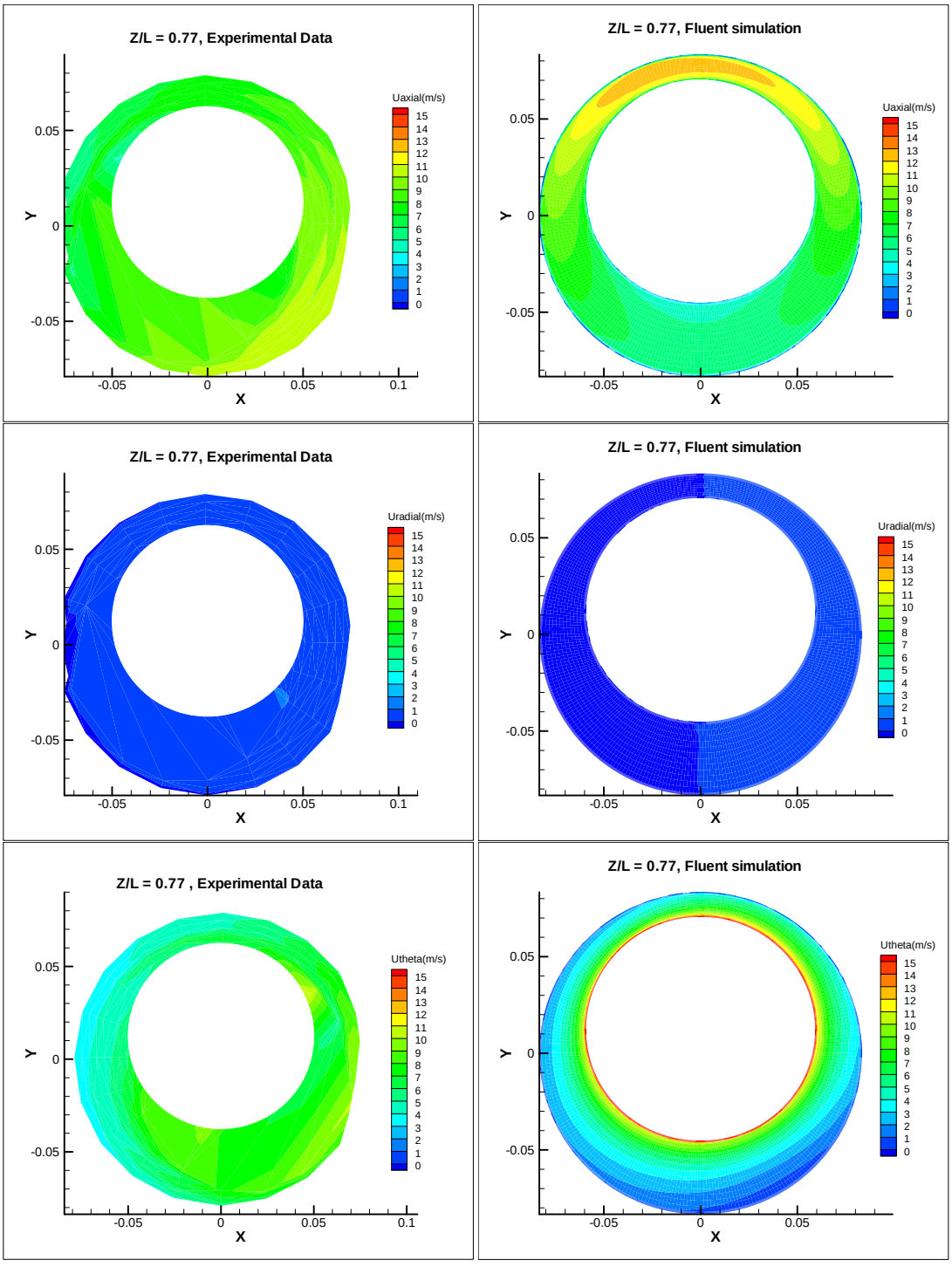

Fig. 5 (d) LDA data and FLUENT simulation results for Z/L = 0.77

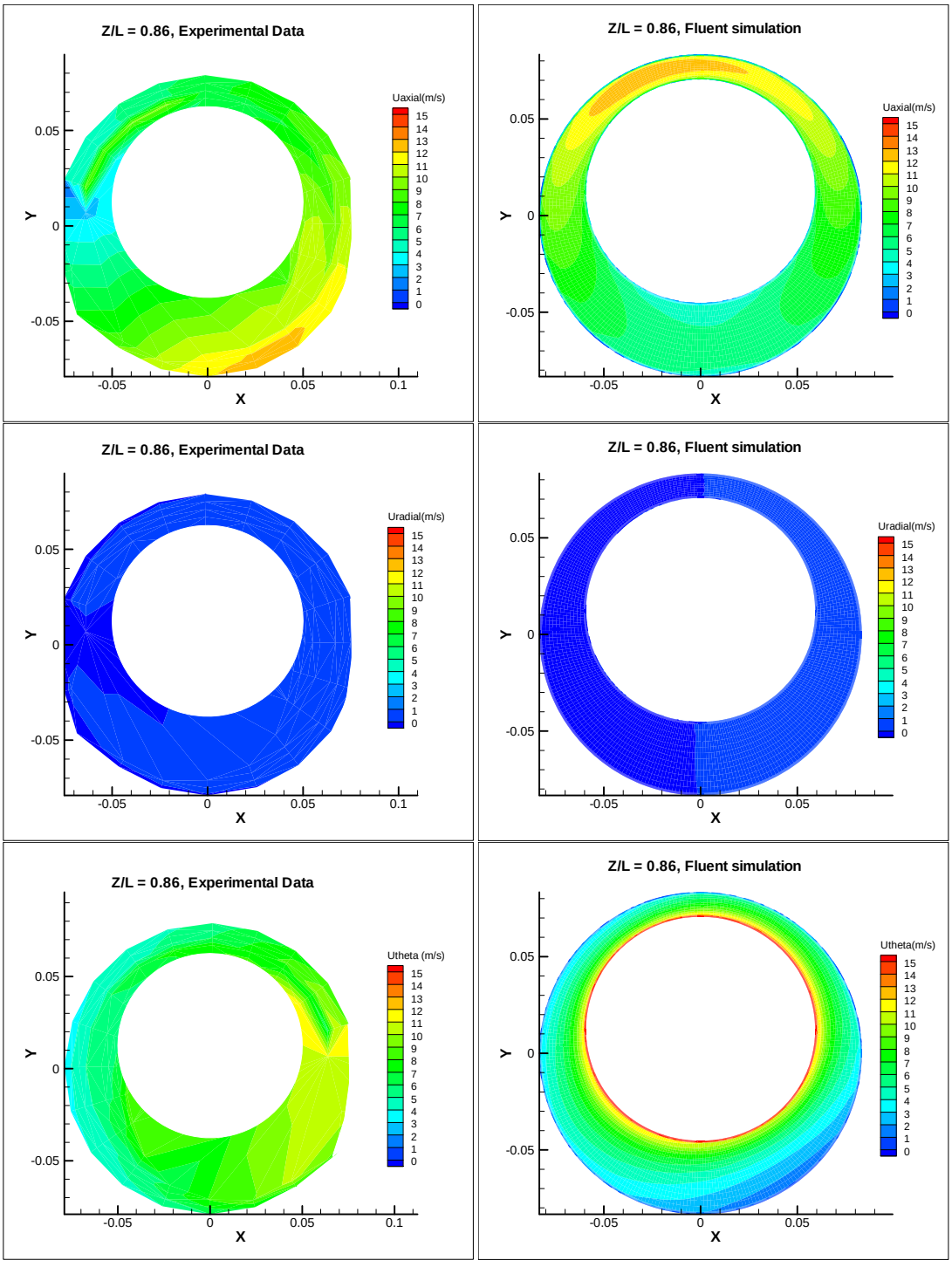

Fig. 5 (e) LDA data and FLUENT simulation results for Z/L = 0.86

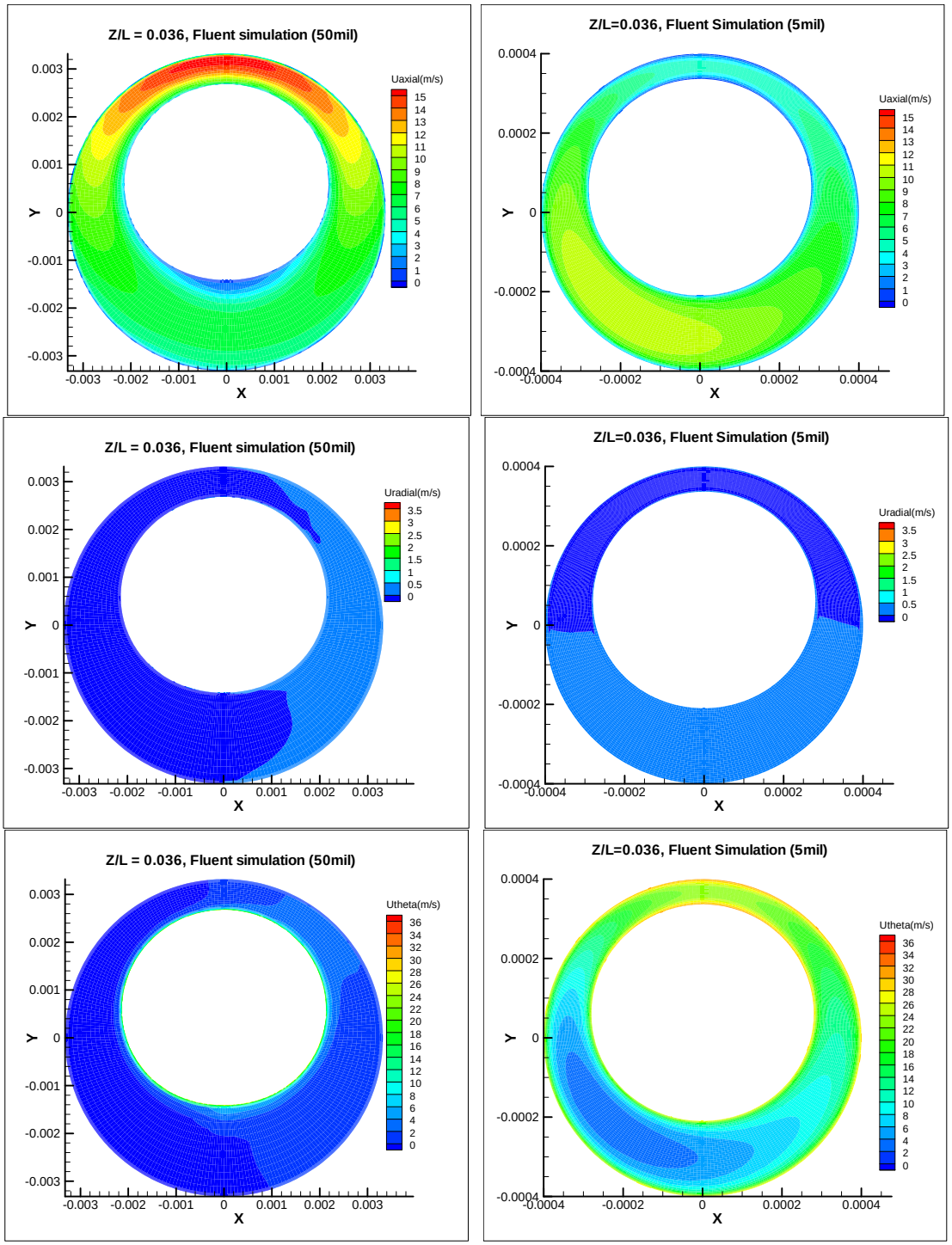

Fig.6 (a) Comparisons of axial, radial and tangential velocity contours for seals of 5 and 50mil clearances at an axial location of Z/L = 0.036

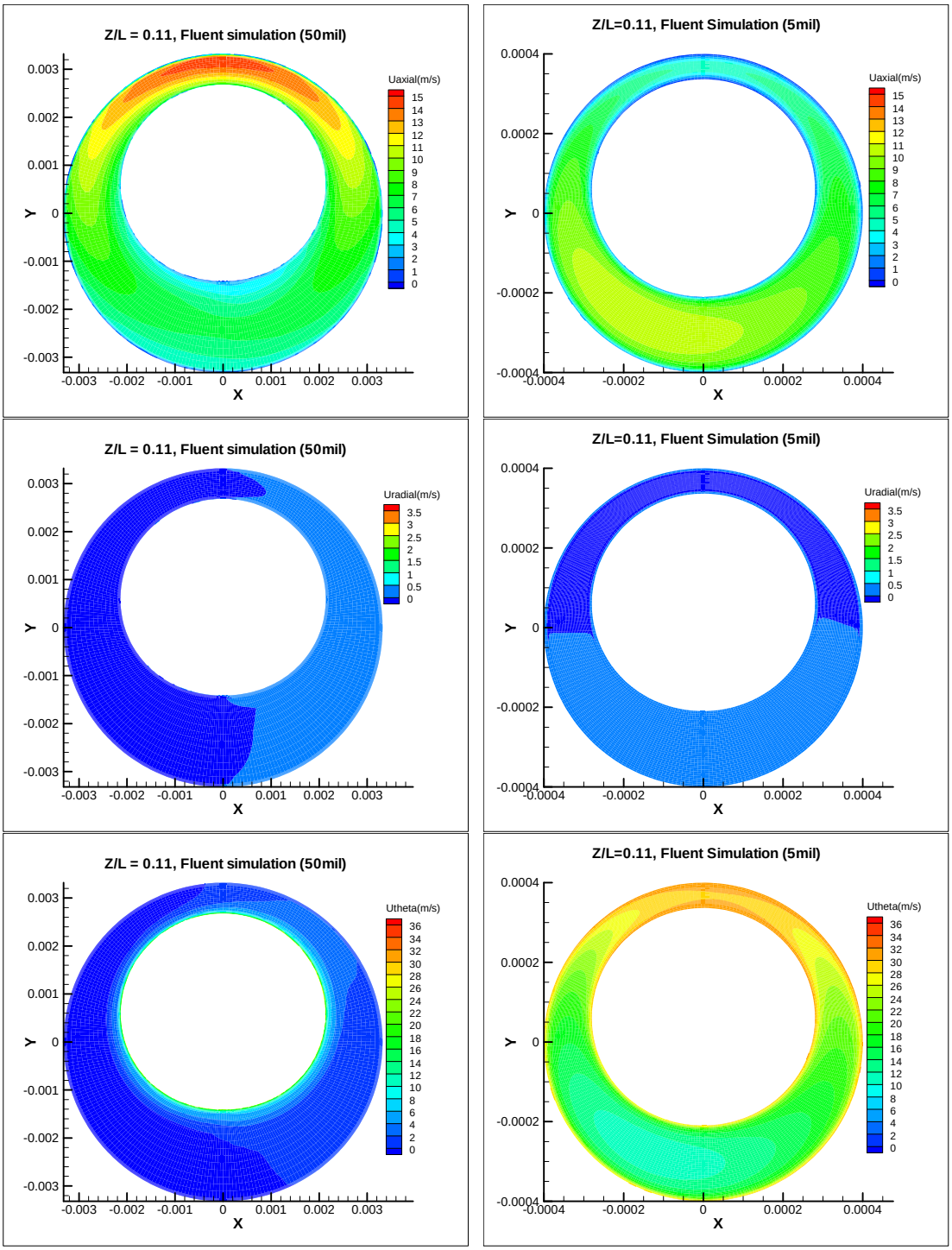

Fig.6 (b) Comparisons of axial, radial and tangential velocity contours for seals of 5 and 50mil clearances at an axial location of Z/L = 0.11

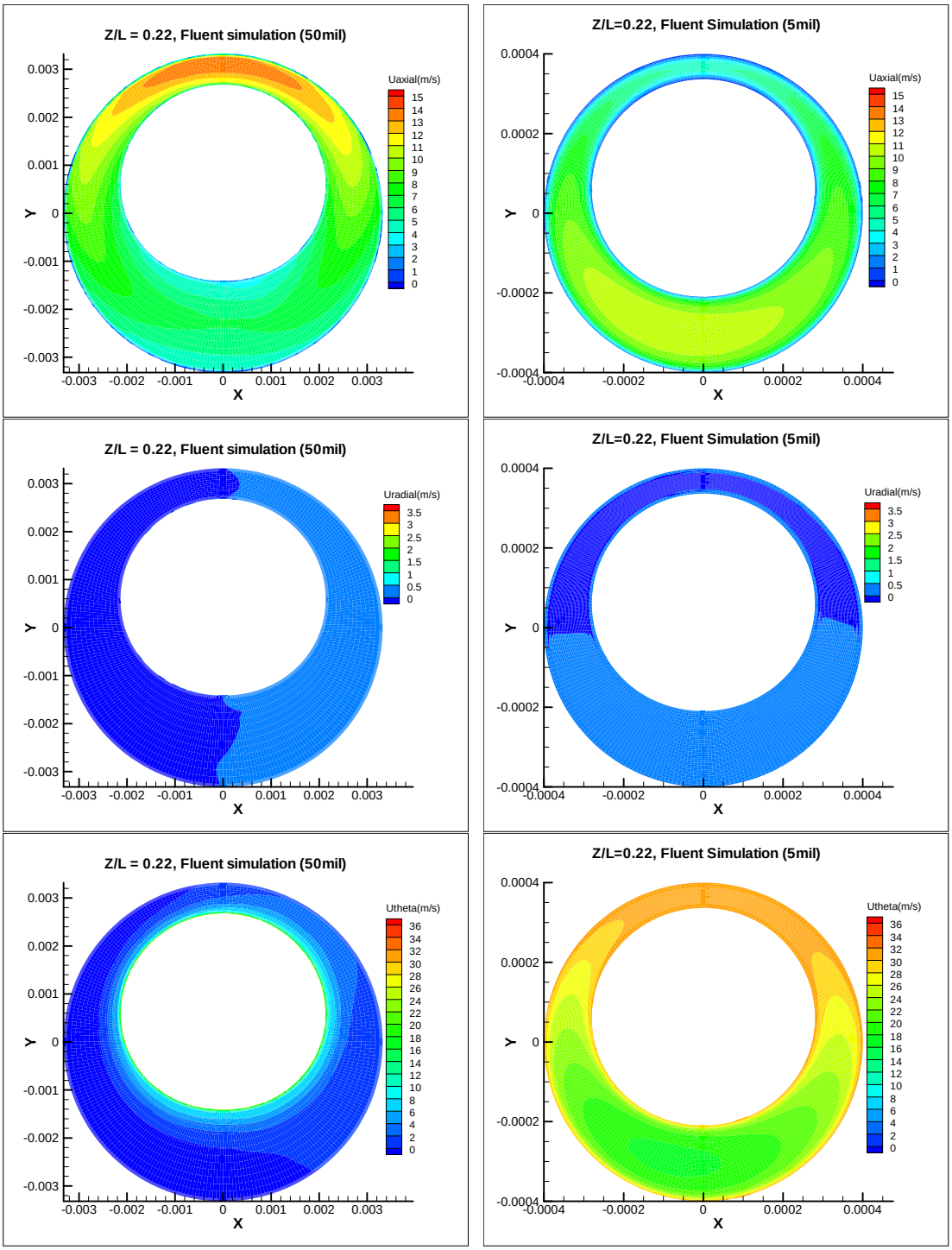

Fig.6 (c) Comparisons of axial, radial and tangential velocity contours for seals of 5 and 50mil clearances at an axial location of Z/L = 0.22

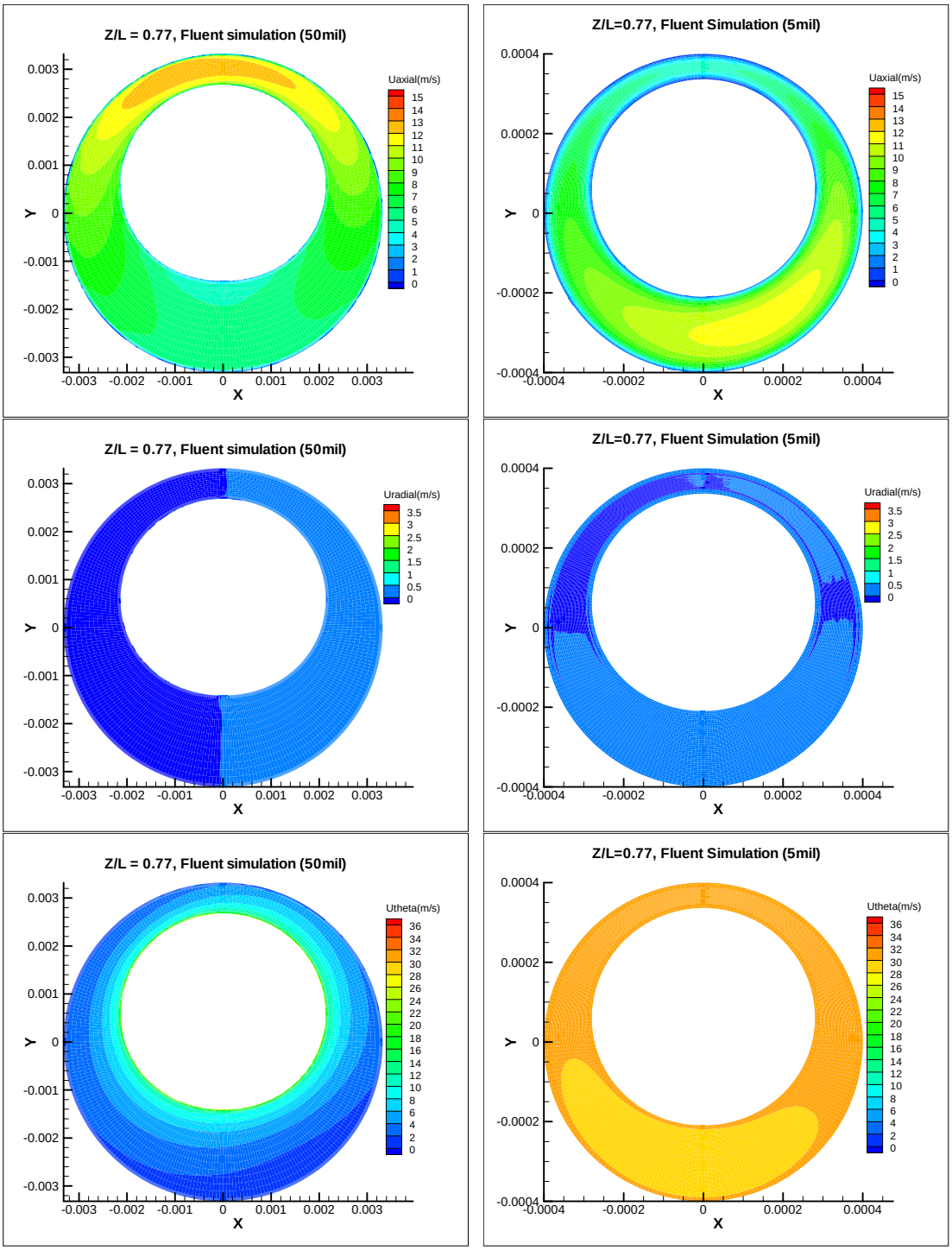

Fig.6 (d) Comparisons of axial, radial and tangential velocity contours for seals of 5 and 50mil clearances at an axial location of Z/L = 0.77

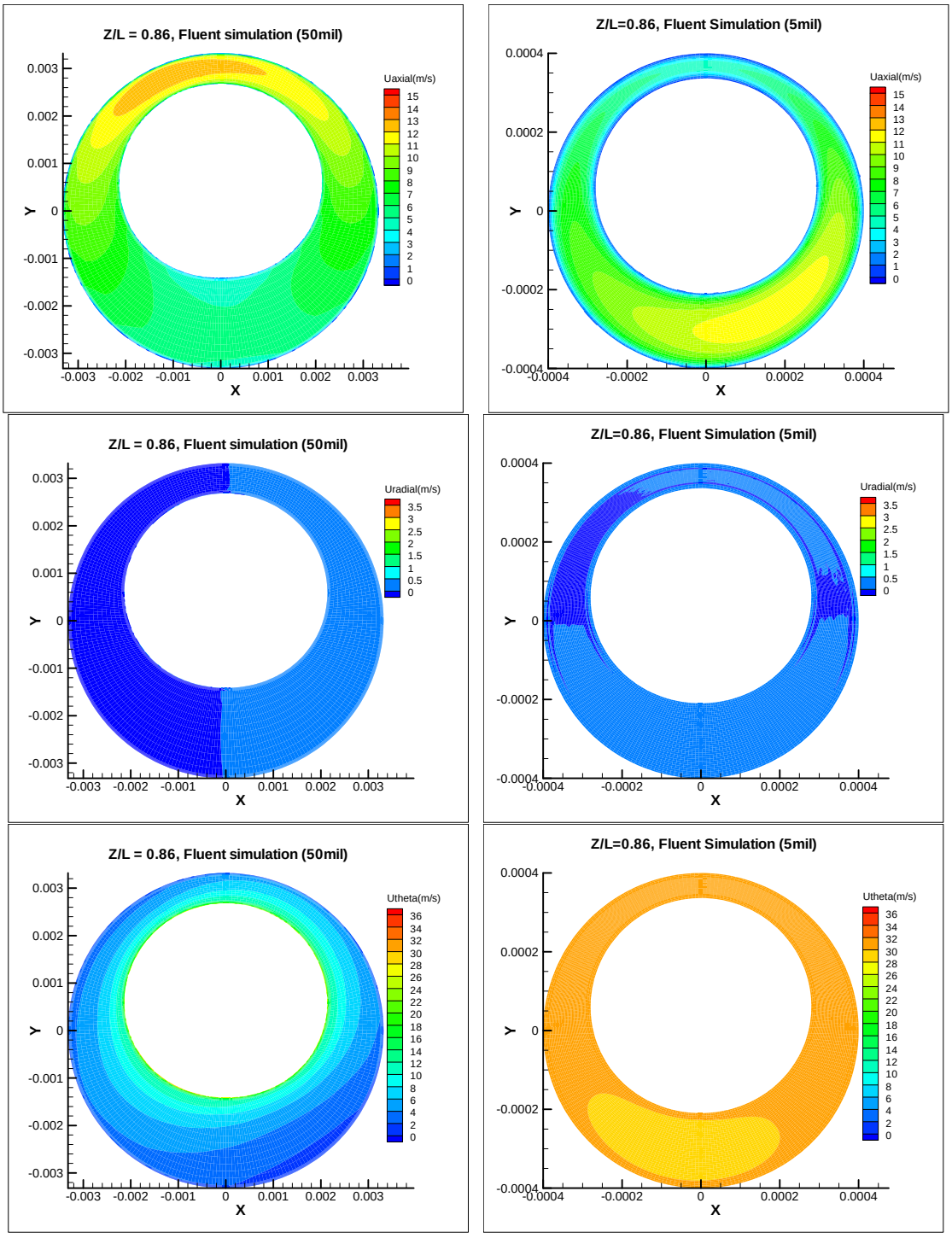

Fig.6 (e) Comparisons of axial, radial and tangential velocity contours for seals of 5 and 50mil clearances at an axial location of Z/L = 0.86

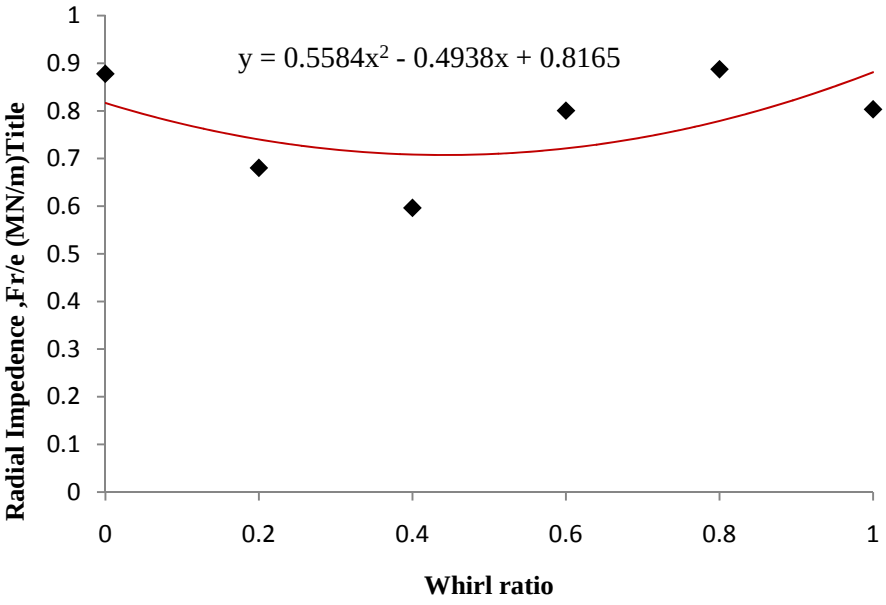

Fig.7 (a) Variation of radial impedance with whirl ratio (50mil)

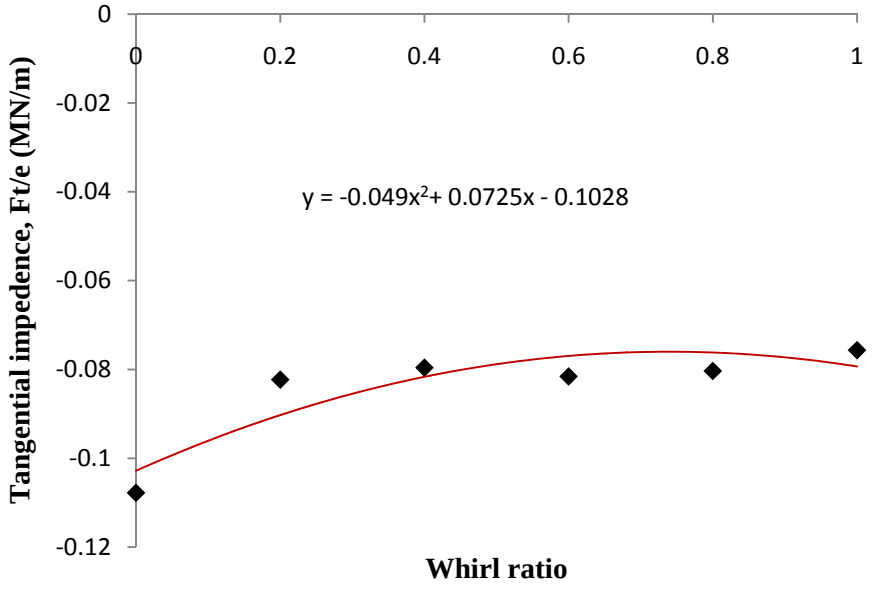

Fig.7 (b) Variation of tangential impedance with whirl ratio (50mil)

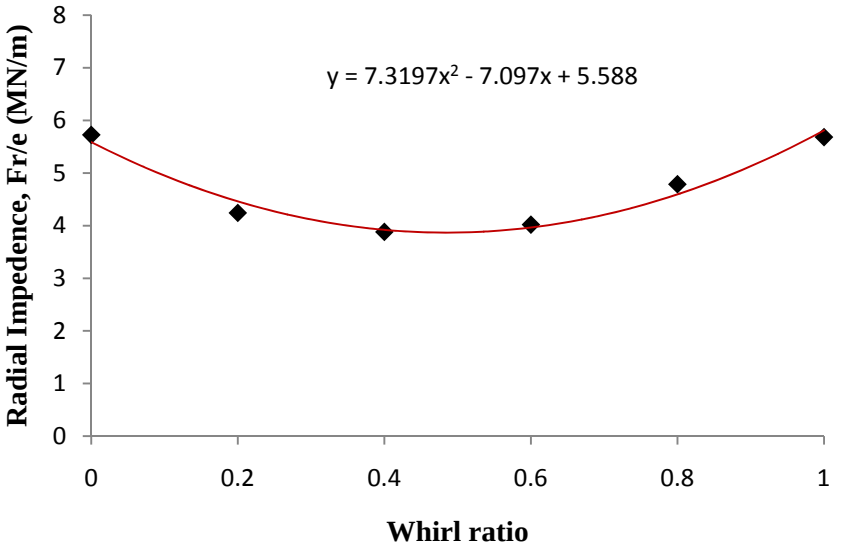

Fig.8 (a) Variation of radial impedance with whirl ratio (5mil)

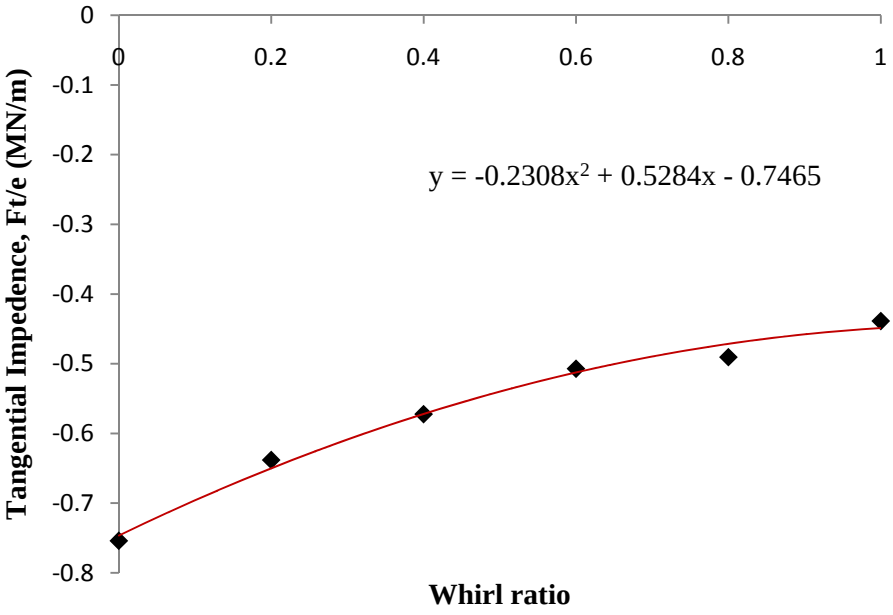

Fig.8 (b) Variation of tangential impedance with whirl ratio (5mil)